



Research article

Source separation of human excreta: Effect on resource recovery via pyrolysis

Maria E. Koulouri^{*}, Michael R. Templeton, Geoffrey D. Fowler

Department of Civil and Environmental Engineering, Imperial College London, SW7 2AZ, UK



ARTICLE INFO

Handling Editor: Jason Michael Evans

Keywords:
 Faecal sludge
 Urine
 Sanitation
 Biochar
 Nutrient
 Energy

ABSTRACT

More people globally are now using on-site sanitation technologies than sewered connections. The management of faecal sludge generated by on-site facilities is still challenging and requires an understanding of all sanitation service chain components and their interactions; from source conditions to treatment and resource recovery. This study aimed to improve the current lack of knowledge regarding these interactions, by establishing a quantifiable relationship between human excreta source separation and resource recovery via pyrolysis. The effects of source separation of faeces and urine on biochar quality were investigated for different pyrolysis temperatures (450 °C, 550 °C, 650 °C) and this information was used to assess energy and nutrient recovery. Results quantify the benefits of urine diversion for nitrogen recovery (70% of total N losses during thermal treatment avoided) and show an increase in the liming potential of the produced faecal-based biochars. The quality of produced solid fuels is also improved when source-separated faeces (SSF) are used as a feedstock for pyrolysis, including a 50% increase in char calorific value. On the other hand, biochars from mixed urine and faeces (MUF) are more rich in phosphorus and potassium, and surface morphology investigation indicates higher porosity compared to SSF biochars. The high salinity of MUF biochars should be considered before agricultural applications. For both biochar types (SSF, MUF), the presence of phosphate compounds of high fertiliser value was confirmed by X-ray diffraction analysis, and temperatures around 500 °C are recommended to optimise nutrient and carbon behaviour when pyrolysing human excreta. These findings can be used for the design of circular faecal sludge management systems, linking resource recovery objectives to source conditions, and vice-versa. Ultimately, achieving consistent resource recovery from human excreta can act as an incentive for universal access to safe and sustainable sanitation.

1. Introduction

Approximately 3.4 billion people rely on on-site technologies to access sanitation services; including pit latrines, septic tanks, composting toilets and container-based sanitation (World Bank, 2019; WHO/UNICEF, 2021). For the first time, this is more people globally than those who use sewered sanitation systems (i.e., flush toilets connected to piped sewer systems). These on-site sanitation facilities produce faecal sludge (FS), which consists of human excreta (faeces and urine) with or without the addition of other waste and wastewater streams. The produced FS needs to be safely contained and treated to avoid environmental pollution and protect public health (Strande et al., 2014), but is not just a waste to be safely discharged; it is also a potential source of valuable resources to be recovered (Guest et al., 2009; Pradel et al., 2016). Therefore, it is essential to develop FS management (FSM) systems that

consider all sanitation service chain components and their interactions, from toilet source conditions to treatment technologies and resource recovery.

One option for FS treatment is pyrolysis, the thermochemical conversion of carbonaceous materials in an oxygen-limited environment (Lehmann and Joseph, 2015). Pyrolysis has been established in the treatment of many organic feedstocks, including wood biomass, agricultural waste and sewage sludge (Méndez et al., 2013; Ippolito et al., 2020). The end-products of the process, which include a solid output known as biochar, a bio-oil and gas (syngas), have various re-use possibilities, making pyrolysis a promising technology for resource recovery research (Somorin et al., 2020; Das and Ghosh, 2021). Although it has not been widely applied for FS treatment, interest in FS pyrolysis is increasing with a focus on energy and nutrient recovery from its end-products (Gold et al., 2018; Bleuler et al., 2020).

^{*} Corresponding author.

E-mail addresses: maria.koulouri17@imperial.ac.uk (M.E. Koulouri), m.templeton@imperial.ac.uk (M.R. Templeton), g.fowler@imperial.ac.uk (G.D. Fowler).

<https://doi.org/10.1016/j.jenvman.2023.117782>

Received 21 November 2022; Received in revised form 13 March 2023; Accepted 19 March 2023

Available online 2 April 2023

0301-4797/© 2023 The Authors. Published by Elsevier Ltd. This is an open access article under the CC BY license (<http://creativecommons.org/licenses/by/4.0/>).

So far, significant progress has been made towards achieving better understanding of FS composition and its distribution among different toilet types and containment systems (Krueger et al., 2021a), as well as establishing standardised methods of FS sampling and analysis (Velkushanova et al., 2021). Previous research has shown that FS composition is very variable and therefore, ensuring uniform treatment standards and consistent quality of recovered products is challenging (Strande et al., 2018). Similar issues have been faced with other types of waste, such as municipal solid waste, and source control has been crucial in achieving consistent recovery of marketable end-products (World Bank, 2012). For FS, source separation of human excreta has often been reported as being beneficial for treatment efficiency and resource recovery (Chipako and Randall, 2020; Larsen, 2020). However, the investigation of how a specific parameter, like source separation, affects FS and end-product characteristics cannot easily be quantified based on existing knowledge, as there are many influencing parameters that are challenging to monitor for on-site sanitation systems. For example, a previous study that compared FS from ventilated improved pit latrines (VIPs) and urine-diverting dry toilets (UDDTs) did not observe significant differences in nutrient content and noted that the studied UDDTs are often not used correctly and likely include urine inputs (Krueger et al., 2021a).

Therefore, there is a necessity to consider how source control can be better deployed in future FSM systems to enable improved treatment and resource recovery efficiency, without assuming that current designs should be replicated. The impact of such work can be significant, as currently 2.4 billion people have access to on-site sanitation that is not safely managed (WHO/UNICEF, 2021). In order to meet the United Nations (UN) Sustainable Development Goal (SDG) 6 on “Clean Water and Sanitation”, FSM services to accommodate these needs have to be secured by 2030, creating an opportunity to inform the design of new sanitation systems to be focused on resource recovery. For this, the connection between source conditions, treatment efficiency and resource recovery should be understood, and source control strategies employed systematically.

This study aimed to quantify the effects of source separation of faeces and urine on resource recovery via pyrolysis by: 1) characterising the two excreta components (separately and combined), while maintaining other influencing parameters of composition, apart from source separation, constant; and 2) assessing biochars from source-separated faeces (SSF) and mixed urine and faeces (MUF) produced at different temperatures (450 °C, 550 °C, 650 °C) for their resource recovery potential. This encompassed the characterisation of SSF and MUF samples for their thermal properties and elemental composition, and the assessment of the effect of pyrolysis temperature on biochar stability. The produced biochars were fully characterised for properties related to soil amendment and solid fuel applications, including the examination of their crystalline composition and surface morphology. While this study deployed pyrolysis as the treatment technology under investigation, presented findings can be used to inform other thermal treatment technologies that may benefit from urine diversion. At a higher level, this work can inform the design of new circular sanitation systems, taking all FSM components under consideration, from the source to the envisioned end-products.

2. Materials and methods

2.1. Human excreta sample collection and preparation

Samples of source-separated faeces and urine were collected from 12 volunteers over a period of 4 months (September to December 2021), at Imperial College London. Ethical approval was received from the Research Governance and Integrity Team of the College (21IC6817) and samples were obtained in line with the Imperial College Healthcare Tissue Bank (ICHTB) process. Ten of the volunteers were non-vegetarian and two mainly followed a vegetarian diet. The detailed sampling

protocol developed for this study is described in Supplementary Material (Appendix S1).

Samples of source-separated faeces (SSF) were dried to constant weight at 105 °C, and dry-sterilised at 150 °C for 150min as suggested by Krueger et al. (2021a). Dry samples were mechanically mixed, homogenised and ground to <10 mm using pestle and mortar. Samples were combined into a composite SSF sample before pyrolysis experiments, both to increase sample representativeness (US EPA, 1995) and to ensure confidentiality of volunteers.

To prepare mixed samples of urine and faeces (MUF), urine samples were collected and stored at 4 °C for up to 1 week before being blended with raw faeces at a ratio of 1g:10 mL (faeces:urine). This ratio is considered representative of the ratio of daily excretion (Rose et al., 2015) and that reported for on-site sanitation systems (Kroumbi et al., 2019). Mixed samples were then dried, dry-sterilised, ground and combined into a homogenised composite MUF sample, following the same procedure as for SSF samples.

2.2. Pyrolysis experiments

The experimental configuration for pyrolysis experiments is illustrated in Fig. S4 (Appendix S2, Supplementary Material). Slow pyrolysis was carried out on a rotary furnace (Carbolite, UK) consisting of a quartz glass reactor connected to an oil trap and condenser. A 30g sample aliquot was placed in the reactor and N₂ was purged at a flowrate of 1.5L/min to ensure an inert atmosphere is maintained. A preliminary assessment showed that a high gas flow rate is optimum for this type of laboratory-scale reactor to ensure that evolving gases are evacuated and do not condense inside the furnace.

The experiments were conducted for two types of feedstocks (SSF, MUF) and three prescribed temperatures (450 °C, 550 °C, 650 °C) at a heating rate of 10 °C/min for 30min. The chosen operational parameters were based on previous research for FS (Liu et al., 2014; Ward et al., 2014; Woldetsadik et al., 2017) and a preliminary thermogravimetric assessment (Appendix S3) that showed no significant change in weight loss after 30min retention time for all the highest heating temperatures tested. All experiments were performed in triplicate and average values are reported. The produced biochars are referred below as SSF450, SSF550, SSF650 and MUF450, MUF550, MUF650, based on the combination of feedstock type and pyrolysis temperature used.

2.3. Analytical methods

Thermal analysis of samples was conducted on a simultaneous thermal analyser (STA) 449 F5 Jupiter (NETZSCH, Germany) to obtain the thermogravimetric analysis (TGA) and derivative thermogravimetry (DTG) curves under 50 mL/min N₂ flow. Proximate analysis was conducted for the determination of volatile matter, fixed carbon and ash content, following standard method ASTM D7582-15 (ASTM, 2015) as adapted by Krueger et al. (2021a) for implementation by TGA. The higher heating value (HHV) was determined by bomb calorimetry, following standard method ASTM D5865/D5865M-19 (ASTM, 2019) on a 6100 Calorimeter (Parr, USA). CHNS analysis was performed on a ThermoScientific Flash Smart Elemental Analyzer according to BS EN ISO 16948:2015 (ISO, 2015). The structure of the biochar and feedstock materials was investigated by Fourier-transform infrared spectroscopy (FTIR). The FTIR spectra were collected based on ASTM E1252-98 (ASTM, 2021), on a Nicolet 6700 FTIR Spectrometer (Thermo Fisher Scientific USA) over the wavenumbers range 4000–500 cm⁻¹, using a diamond ATR-crystal.

Analysis of the inorganic constituents of samples was performed by ICP-OES (Inductively Coupled Plasma Optical Emission Spectroscopy) on an Avio 500 (PerkinElmer, USA). The samples were first dry-ashed at 490±5 °C for 4 h (APHA, 1992; Hseu, 2004) and then digested with aqua regia for 2 h at 95 °C, based on Standard Method 3050B (US EPA, 1996) as adapted by Krueger et al. (2020). Availability of phosphorus (P) was

determined after overnight extraction by 2% formic acid (Wang et al., 2012; IBI, 2015).

The pH and electrical conductivity (EC) of biochars were measured at a 1:20 ratio (biochar:H₂O [g:mL]) after mechanical shaking for 1h (Singh et al., 2017). The biochar liming potential was determined as CaCO₃-equivalency by adding 10 mL standardised 1M HCl to 0.5g of sample, shaking for 2 h and leaving the mixture to stand overnight. The solution was then titrated with standardised 0.5M NaOH until pH 7 was reached (Singh et al., 2017). Cation exchange capacity (CEC) was determined by saturating the biochar sample with a 1M NH₄OAc solution (at pH 7) overnight, followed by washing with ethanol and addition of 1M KCl to displace the NH₄⁺ exchangeable cations (Chapman, 1965).

Ammonium concentration in the final extract was analysed using a Skalar auto-analyser (Skalar Analytical BV).

The crystalline phases of biochar samples were analysed by X-ray diffraction (XRD) using a Bruker AXS D8 Advance system with a non-monochromated Cu K α radiation source, with an average $\lambda = 1.504 \text{ \AA}$ over a scanning range of 10–90° (2 θ range). The phase determination was performed using in-built High Score Plus X'Pert software methods (Malvern Panalytical). The surface morphology of the biochars was analysed under field-emission scanning electron microscopy (SEM) on a TM4000 Tabletop Microscope (Hitachi, Japan).

A flowchart summarising the study methodology is included in Appendix S2. Samples were manually ground to <2 mm for pH, EC, CaCO₃-

Table 1

Physical and chemical characterisation (on a dry basis) of biochars produced from source-separated faeces (SSF) and mixed human excreta (MUF) at different pyrolysis temperatures (450 °C, 550 °C, 650 °C). Mean values presented from analyses performed in triplicate (standard deviation in brackets).

Parameter	Unit	Feedstocks		SSF biochars			MUF biochars			Guidelines (max. allowed values)	
		SSF	MUF	450 °C	550 °C	650 °C	450 °C	550 °C	650 °C	EBC (2012)	IBI (2015)
Char yield	[%]			34.4 (±0.5)	31.1 (±0.5)	29.4 (±0.2)	45.5 (±0.9)	41.7 (±0.9)	38.5 (±0.6)		
VM	[%]	72.5 (±0.6)	70 (±0.2)	24.4 (±1.7)	14.8 (±0.3)	12.9 (±1.5)	27.0 (±0.1)	18.8 (±1.2)	15.0 (±0.3)		
FC	[%]	15.1 (±0.3)	11.2 (±0.3)	43.0 (±0.7)	50.5 (±0.6)	50.1 (±0.7)	22.9 (±0.6)	26.4 (±0.7)	28.7 (±0.3)		
Ash	[%]	12.5 (±0.4)	18.9 (±0.5)	32.6 (±0.7)	34.7 (±0.6)	37.0 (±0.3)	50.1 (±0.6)	54.8 (±0.5)	56.3 (±0.2)		
HHV	[MJ/kg]	21.8 (±0.1)	17.8 (±0.0)	20.3 (±0.1)	17.9 (±0.4)	17.7 (±0.3)	13.3 (±0.3)	12.3 (±0.5)	12.3 (±0.1)		
C	[%]	50 (±0.4)	41 (±0.8)	50.9 (±0.6)	50.4 (±0.3)	48.8 (±0.6)	33.1 (±0.6)	32.2 (±0.9)	32.2 (±0.4)		
H	[%]	6.8 (±0.2)	5.3 (±0.2)	3.3 (±0.0)	1.8 (±0.0)	1.3 (±0.0)	1.9 (±0.1)	1.1 (±0.0)	0.8 (±0.0)		
N	[%]	4.9 (±0.2)	6.8 (±0.3)	4.7 (±0.0)	4.5 (±0.1)	4.3 (±0.1)	4.9 (±0.0)	4.4 (±0.1)	4.0 (±0.1)		
S	[%]	1.3 (±0.1)	2.1 (±0.4)	1.2 (±0.0)	<0.1	<0.1	2.0 (±0.1)	1.4 (±0.3)	0.8 (±0.0)		
H:C ratio	–			0.77	0.43	0.32	0.68	0.41	0.30		
pH	–			9.6 (±0.0)	10.4 (±0.1)	11.2 (±0.1)	9.2 (±0.1)	10.4 (±0.0)	10.6 (±0.1)		
EC	[mS/cm]			2.7 (±0.2)	3.5 (±0.1)	4.9 (±0.2)	28.8 (±0.8)	29.2 (±0.4)	28.8 (±0.4)		
CaCO ₃ -eq.	[%]			12.2 (±0.3)	13.2 (±0.4)	13.0 (±0.3)	5.3 (±0.2)	8.2 (±0.4)	11.4 (±0.5)		
CEC	[cmol/kg]			69.6 (±0.7)	40.1 (±1.0)	24.8 (±1.1)	73.8 (±0.6)	47.8 (±1.0)	46.0 (±3.0)		
P	[g/kg]	22.4 (±0.1)	32.2 (±0.5)	50.9 (±0.0)	55.1 (±1.7)	58.3 (±1.4)	58.7 (±0.9)	64.4 (±0.0)	66.8 (±2.7)		
P (2% FA)	[g/kg]			49.1 (±1.1)	53.0 (±1.6)	50.3 (±1.0)	56.0 (±0.3)	61.7 (±0.1)	62.5 (±0.1)		
	[% P]			96.6	96.1	95.5	95.5	95.8	93.6		
K	[g/kg]	12.9 (±0.1)	28.5 (±0.2)	45.3 (±1.4)	48.6 (±1.5)	51.9 (±1.1)	74.5 (±0.7)	84.8 (±1.9)	84.8 (±0.2)		
Ca	[g/kg]	23.2 (±0.1)	17.7 (±0.1)	53.9 (±1.3)	59.4 (±2.2)	63.9 (±2.0)	40.3 (±1.1)	41.4 (±0.7)	43.2 (±1.4)		
Mg	[g/kg]	8.8 (±0.1)	8.7 (±0.1)	20.6 (±0.3)	22.9 (±0.5)	24.6 (±1.3)	16.8 (±0.1)	18.4 (±1.3)	19.4 (±1.7)		
B	[mg/kg]			34.6 (±1.6)	34.1 (±0.1)	39.6 (±3.9)	83.2 (±0.1)	83.6 (±3.6)	86.8 (±0.8)		
Zn	[mg/kg]			443.5 (±31.5)	449.4 (±14.4)	535.0 (±41.0)	245.3 (±2.0)	260.5 (±5.6)	263.1 (±3.6)	400	416–7400
Mn	[mg/kg]			318.9 (±10.4)	322.0 (±24.7)	353.7 (±17.0)	188.9 (±5.5)	202.3 (±8.6)	205.7 (±18.3)		
Fe	[mg/kg]			739.3 (±20.1)	752.8 (±23.9)	792.6 (±38.2)	492.3 (±42.9)	462.7 (±12.1)	468.5 (±10.2)		
Cu	[mg/kg]			120.4 (±3.1)	122.3 (±1.1)	135.7 (±6.1)	81.7 (±1.8)	88.7 (±0.4)	90.9 (±0.1)	100	143–6000
Ba	[mg/kg]			25 (±3.3)	24.7 (±2.0)	27.8 (±2.2)	4.8 (±0.5)	6.2 (±1.7)	3.8 (±1.2)		
Cd	[mg/kg]			<20	<20	<20	<20	<20	<20	1–1.5	1.4–39
Co	[mg/kg]			<20	<20	<20	<20	<20	<20		34–100
Cr	[mg/kg]			<20	<20	<20	<20	<20	<20	80–90	93–1200
Pb	[mg/kg]			<20	<20	<20	<20	<20	<20	120–150	121–300

VM = Volatile matter, FC = Fixed carbon, HHV = Higher heating value, CaCO₃-eq. = Calcium carbonate equivalency, P (2% FA) = 2% formic acid extractable P, EBC = European Biochar Certificate, IBI = International Biochar Initiative.

eq. and CEC determination and $<500 \mu\text{m}$ for all other analytical procedures. All analyses were performed in triplicate and results are presented as mean values. Standard deviation values are presented in brackets, where available. Results were statistically analysed by two-way ANOVA (using MATLAB) to investigate the influence of source separation and pyrolysis temperature on biochar characteristics, at the 0.05 significance level. Multiple comparison tests were used to localise the impact of pyrolysis temperature, where a significant influence was detected.

3. Results & discussion

3.1. Human excreta characterisation

Feedstock characteristics are summarised in Table 1. Proximate analysis showed higher content of fixed carbon for SSF compared to MUF (15.1% and 11.2% respectively) and the opposite trend for ash content (12.5% and 18.9% respectively). The higher ash content of MUF can be attributed to the presence of inorganic salts in urine (Rose et al., 2015). The measured calorific value is also higher for SSF compared to MUF (21.8 MJ/kg compared to 17.8 MJ/kg) showing that source-separated faeces are a more energy-dense feedstock. MUF are higher in nitrogen (N) (6.8% compared to 4.9% for SSF) as well as P and K, which is expected, as most of the nutrients excreted from the human body are found in urine (Larsen et al., 2013). These results are expressed on a dry basis, so N volatilisation during thermal drying is expected for both feedstocks. Ca content is relatively higher for SSF, and Mg is almost equally distributed between the two excreta streams. Nutrient concentrations in fresh urine are included in Appendix S4.

The urine fraction significantly increased the volume and moisture of FS to $>90\%$ initial moisture content. Source separation can therefore reduce the need for mechanical dewatering before pyrolysis, which largely influences the energy efficiency of FS pyrolysis systems (Bond et al., 2018). Low-cost drying methods, including solar drying, can be used for SSF feedstocks, which had a median initial moisture content of approximately 75%. The efficiency of these methods is case-specific and can be dependent on the geographical location (Liu et al., 2014).

Further structural differences between the two sample groups were investigated by FTIR spectroscopy. FTIR has been suggested as a quick method to measure faecal fat content, mainly by identifying regions of fatty acids (De Koninck et al., 2016). Typical peaks of aliphatic C–H bonds appearing at 2920 and 2850 cm^{-1} are almost identical for SSF and MUF (Fig. 1), as the fat content in human excreta sludges is attributed to the faecal stream. A distinct shoulder peak also appears for SSF at $\sim 1745 \text{ cm}^{-1}$ which can be related to the presence of lipids (C=O stretching). Some additional differences in frequency were observed within the $1750\text{--}1550 \text{ cm}^{-1}$ range, which can be attributed to the difference in protein structure when urine is present, as amide and peptide bonds form strong peaks within this region (Haris and Severcan, 1999).

Both sample groups show a broad peak at $3700\text{--}3100 \text{ cm}^{-1}$ (O–H stretching) and a strong peak at $1200\text{--}950 \text{ cm}^{-1}$ (C–O and C–C stretching, linked to carbohydrates) which have previously been observed for FS (Krueger et al., 2021b). The latter peak at $1200\text{--}950 \text{ cm}^{-1}$, as well as the peak forming around 500 cm^{-1} have also been attributed to the presence of phosphates (Jastrzębski et al., 2011; Shapaval et al., 2019).

Thermal analysis results (Fig. 2) show the differences in decomposition behaviour when urine is present, compared to source-separated faeces. Three thermal decomposition stages are observed within the typical pyrolysis temperature range ($200\text{--}700 \text{ }^\circ\text{C}$) for both sample groups. Similar stages have been observed by previous studies for human excreta (Somorin et al., 2020) and FS (Krueger et al., 2021b). This study provides a deeper understanding of how source separation impacts decomposition behaviour.

The three identified stages in Fig. 2 are as follows:

1) $200\text{--}400 \text{ }^\circ\text{C}$

Rapid weight loss ($>50\%$ of initial weight) mainly attributed to the decomposition of protein, hemicellulose, cellulose and other carbohydrates (Krueger et al., 2021b). The maximum weight loss rate peak is observed at $310 \text{ }^\circ\text{C}$ for SSF, while for MUF it is observed at $320 \text{ }^\circ\text{C}$ and preceded by a smaller peak between 250 and $290 \text{ }^\circ\text{C}$. This different pattern may be attributed to the decomposition of urea-based nitrogenous compounds in mixed excreta sources (Jones and Rollinson, 2013; Zhu et al., 2021).

2) $400\text{--}550 \text{ }^\circ\text{C}$

Weight loss within this temperature range has been attributed to the completion of lignin decomposition reactions and to the cracking of oil and grease (Krueger et al., 2021b). A distinct shoulder is observed on the DTG curves, occurring at around $450 \text{ }^\circ\text{C}$ until the completion of main pyrolytic reactions by $550 \text{ }^\circ\text{C}$. Similar findings have been reported by Fidalgo et al. (2019) for human faeces. Here, it can further be observed that this shoulder is more distinct for SSF compared to mixed excreta, due to the excretion of dietary fat through the faecal stream.

3) $>550 \text{ }^\circ\text{C}$

During the final stage, and for temperatures $>550 \text{ }^\circ\text{C}$, gradual weight loss occurs due to continued carbonisation. At temperatures higher than $700 \text{ }^\circ\text{C}$ further weight loss occurs, which can be attributed to the decomposition of inorganic compounds, including carbonates (Kwon et al., 2018). Notably, these occur at a significantly higher rate for urine-containing excreta sources, which can be attributed to the high presence of inorganic salts in urine (Rose et al., 2015).

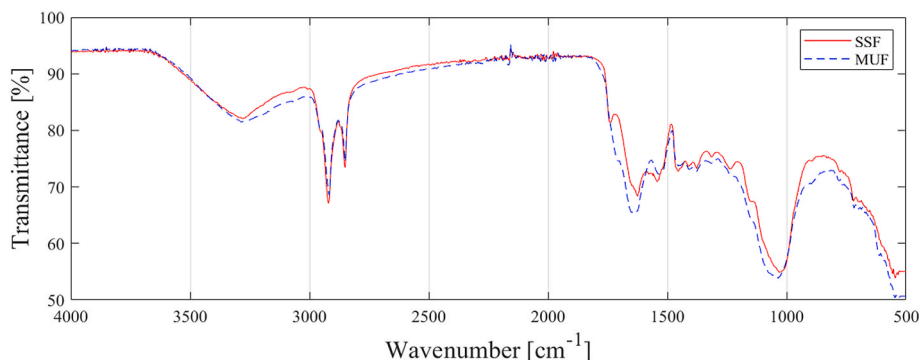


Fig. 1. Fourier-transform infrared spectroscopy (FTIR) spectra for source-separated faeces (SSF) and mixed human excreta (MUF).

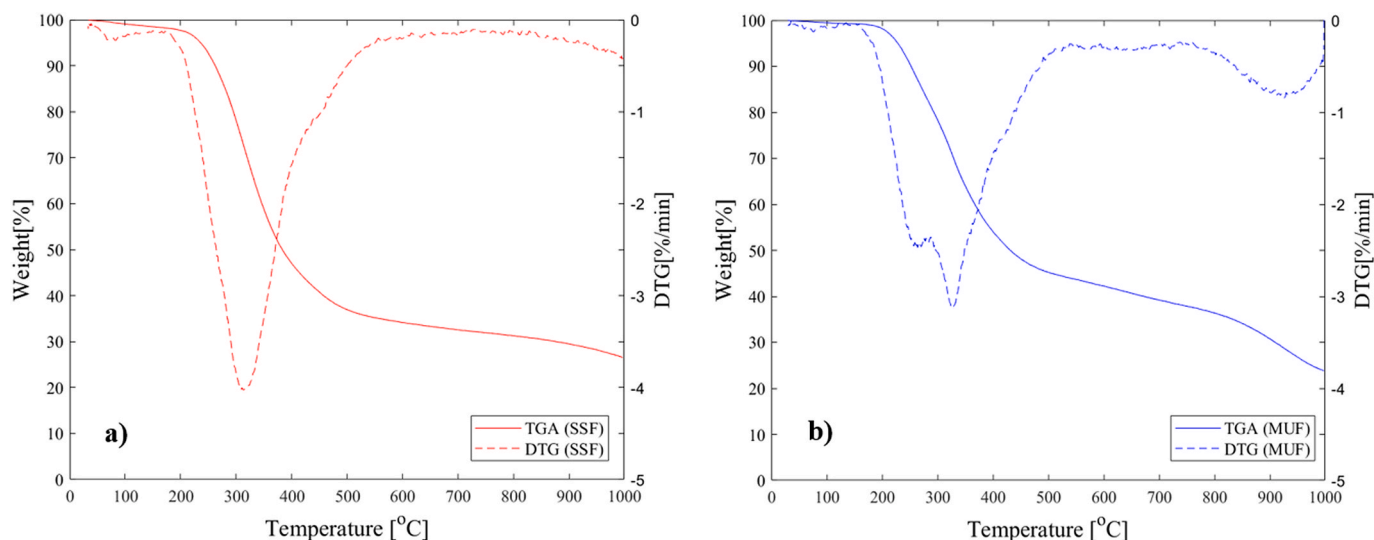


Fig. 2. Thermogravimetric analysis (TGA) and derivative thermogravimetry (DTG) curves for source-separated faeces (SSF) (a) and mixed human excreta (MUF) (b).

3.2. Biochar stability

According to the International Biochar Initiative (IBI) and European Biochar Certificate (EBC) guidelines, the H:C molar ratio can be used as an indicator of biochar stability. Biochars with H:C < 0.7 are recommended as stable, as this indicates the prevalence of fused aromatic string structures, while H:C > 0.7 indicates that pyrolytic reactions have not been completed (EBC, 2012; IBI, 2015). This requirement is met for excreta-derived biochars produced at 550 °C or higher temperatures, while at 450 °C the H:C ratio is 0.8 for SSF and 0.7 for MUF (Table 1). Previous studies that tested FS-derived chars produced at 500 °C reported H:C < 0.7, indicating complete pyrolytic reactions at this temperature (Liu et al., 2014; Krounbi et al., 2018). Therefore, biochar stability during human excreta pyrolysis is expected to be achieved between 450 and 500 °C.

These findings were confirmed by FTIR analysis for the biochars produced (Fig. S5, Appendix S5). Notably, some vibrations at 3000–2800 cm⁻¹, which are linked to aliphatic C–H bonds present in the feedstock materials, were still observed for biochars produced at 450 °C, particularly for SSF which had the highest H:C ratio at this temperature. These aliphatic methylene bands have been suggested as an indication of the level of decomposition of organic wastes (Smidt and Schwanninger, 2005). Similar results for sewage sludge-derived chars have shown that these peaks disappear at temperatures ≥500 °C (Ren et al., 2018).

Therefore, temperatures around 500 °C are recommended for human excreta pyrolysis applications, particularly those involving environmental exposure (e.g., use of the biochar in agriculture). Further optimisation should be performed on a case-specific basis, as the optimum temperature would be influenced by several factors, including feedstock mass and furnace size.

3.3. Biochar characterisation

Biochar characteristics are summarised in Table 1. ANOVA results (Appendix S6) suggest that source separation has a significant ($p < 0.05$) effect on all tested parameters. The char yield is higher for MUF compared to SSF for all pyrolysis temperatures, although this increase can be attributed to the higher ash content in MUF. Both types of biochar showed a similar volatile matter decrease pattern for the temperatures tested (no significant interaction effects observed between source separation and temperature by ANOVA). The relatively high residual volatile matter content of these biochars (>10%), even after preparation at high pyrolysis temperatures, can be attributed to the method followed

for volatile matter determination (at 950 °C). As discussed for the presented TGA curves (Fig. 2), a second weight loss peak occurs for both feedstocks at high temperatures (>700 °C) due to the decomposition of inorganic compounds. Therefore, an overestimation of the volatile matter can occur for excreta-based feedstocks when using this standard method and should be taken into consideration when interpreting results.

3.3.1. Value as a soil amendment

The measured pH values (>9) show that all the biochars prepared were alkaline. The pH increased alongside the ash content with higher pyrolysis temperatures, similar to previous findings for FS (Liu et al., 2014; Krounbi et al., 2018). A quantifiable parameter often used in agriculture relating to the ability to treat acidified soils is the biochars' liming potential, expressed as CaCO₃ equivalency (Ippolito et al., 2015). In this aspect, a difference is observed between biochar types, with SSF having significantly higher liming potential (p-values in Table S3) despite pH values being similar, particularly at temperatures up to 550 °C. Moreover, the electrical conductivity (EC) of MUF biochars is up to 10 times higher than SSF biochars (Table 1); this is indicative of the large ion concentration present in urine. These ions include saline-causing species, as confirmed by XRD analysis (Fig. 4), so should be taken into consideration particularly for salt sensitive plants that may be negatively affected by high salinity in applied biochars (Bleuler et al., 2020).

Cation exchange capacity (CEC) is also a crucial parameter for soil amendments as it is a measure of a soil's ability to adsorb and retain nutrients in exchangeable forms that are available for plant uptake (Chapman, 1965). CEC was found to decrease with increasing temperature for both sample groups, particularly for SSF, suggesting that lower pyrolysis temperatures (≤500 °C) may be required for improvement of a soil's nutrient-holding capacity from human excreta-derived biochars (Table 1). The same trend has been reported for container-based sanitation FS (Krounbi et al., 2019), while the opposite trend was observed by Gold et al. (2018) for FS from septic tanks and pit latrines, where additional waste inputs are often added and may deviate from the behaviour of human excreta. Gold et al. (2018) also noted the inconsistent influence of pyrolysis temperature on CEC for different types of chars.

The fact that the method used measures CEC at pH 7 needs to be taken under consideration when interpreting these results, as pH-dependent variable charges can influence CEC measurements (Munera-Echeverri et al., 2018). The NH₄OAc extraction method at pH 7 used in

this study is a common standard for comparison between laboratories, however, the high pH and liming potential of the produced biochars might affect their nutrient exchange behaviour when applied to different soils, as generally CEC has been found to increase with increasing pH (Singh et al., 2017).

3.3.2. Nutrient recovery

Nutrient retention is a crucial challenge of resource circularity and the connection between SDG 6 and SDG 2 (“Zero Hunger”) has been established by several studies (Orner and Mihelcic, 2017; Trimmer et al., 2017). Particularly the issue of declining P availability has gained a lot of interest over the past decades as P is a finite, non-substitutable resource that is essential to life and plant growth and, ultimately, food security (Cordell et al., 2009). P and K are generally concentrated in biochars, with MUF providing higher PK concentrations (Table 1), as expected based on the daily excretion ratios of these elements between faeces and urine. P availability (2% formic acid extractable) appears to be very high up to 550 °C and starts declining at 650 °C (Table 1), suggesting that temperatures around 500–550 °C would be best for P availability in excreta-based biochars. These results are in line with previous studies that suggest temperatures <600 °C when producing biochars for use in agriculture (Glaser and Lehr, 2019).

Nitrogen is also an essential macronutrient, and its synthetic production can be very energy-intensive and costly (Canfield et al., 2010). Expressing biochar N content results shown in Table 1 as g/person/day (based on daily excretion ratios presented in Rose et al. (2015)) allows the estimation of N retention for two scenarios: a) a source-separating system, with SSF550 biochar and separated urine (SSU) as its products, and b) a mixed-streams system with MUF550 biochar as its product. It can be calculated that for scenario (a) only 3.2% of total N excreted is retained in the SSF550 biochar and 80% can be retained in source-separated urine. For scenario (b) MUF550 contains only 12.6% of total N excreted, due to volatilisation losses. Therefore, around 70% more N (% of total) is retained and available for recovery through a source-separating system, compared to a mixed-streams scenario (detailed calculations in Appendix S7).

Ca and Mg are concentrated in the biochar and increasing with pyrolysis temperature, but are higher for SSF, in line with excretion ratios and concentrations of the feedstocks. Trace elements concentrations meet IBI standards, while the stricter EBC thresholds are exceeded for Zn and Cu of SSF biochars and are below the detection limit for Cd. Multiple comparison test p-values (Appendix S6) showed significant increase in trace elements concentrations at the 550–650 °C temperature range, suggesting that pyrolysis temperatures below 550 °C could minimise heavy metal concentration in the final products. Heavy metal bioavailability and mobility are expected to be reduced in biochars compared to feedstocks (Hossain et al., 2011; Woldetsadik et al., 2017). For full-scale applications, it is expected that human excreta will be mixed with other biomass sources, either as cover material during containment in toilets or to enhance drying during pre-treatment (e.g., sawdust). Therefore, total heavy metal concentrations are expected to be diluted and should be compared to maximum allowed threshold values in a case-specific context, considering potential country-specific regulations for the intended use(s) of recovered products.

In order to qualitatively investigate the inorganic compounds present, the ash fractions of both biochar types were analysed via FTIR (after ashing at 600 °C for 4h). Results (Fig. 3) show a band peak at 1040–1010 cm^{-1} and another at 650–550 cm^{-1} , which can be attributed to phosphate compounds, including potassium phosphates and calcium phosphates (apatites) (Jastrzębski et al., 2011), as further confirmed by XRD analysis (Fig. 4). For SSF, the bands around 1040 cm^{-1} are forming a more intense peak and there are additional peaks at 1550–1350 cm^{-1} and ~870 cm^{-1} , which are characteristic of carbonates (Jones and Jackson, 1993) and carbonated apatites (Rehman and Bonfield, 1997; Stanislavov et al., 2018). Calcium carbonate can be formed spontaneously in biochars when $\text{Ca}(\text{OH})_2$ (formed when CaO is hydrated) reacts

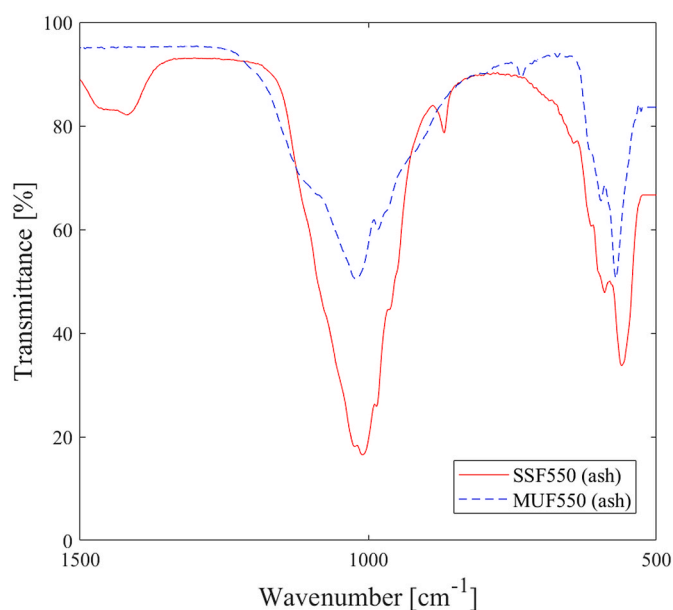


Fig. 3. Fourier-transform infrared spectroscopy (FTIR) spectra for the ash fraction of source-separated faeces (SSF) and mixed urine and faeces (MUF) biochars (produced at 550 °C).

with CO_2 (Galván-Ruiz et al., 2009). The prevalence of carbonates or carbonated apatite in SSF biochars can explain the higher liming potential observed for these biochars and shows their promising soil improvement potential.

XRD analysis confirmed the heterogeneity of the produced biochars, and the observed peak positions (2 θ) were identified as the fingerprint of the crystal phases present (Fig. 4). Both biochar samples are characterised by a broad background diffraction pattern indicative of amorphous silica (Singh et al., 2017), while the broad peaks observed for SSF550 indicate the stacking structure of aromatic layers in the biochar and validate the carbon-rich nature of the sample (Takagi et al., 2004). MUF550 biochar shows mostly distinctive, sharp peaks due to the prevalence of inorganic compounds.

Sharp diffraction peaks observed for both samples match the pattern of KCl salts (Ismail et al., 2022) and are more intense for MUF compared to SSF biochars. The presence of NaCl salts is also observed for MUF550, confirming the stronger salinity of mixed excreta biochars, which may place limitations on their use in agriculture (Bleuler et al., 2020). Similar diffraction peaks have been attributed to the formation of calcium sulphide crystals, suggesting that the S present in MUF biochars may bound Ca ions. Both samples included peaks attributed to the presence of potassium, magnesium and calcium phosphates. The high concentration of P in both samples (Table 1) suggests that amorphous phosphorous compounds are also present in the biochars (Figueiredo et al., 2021).

For SSF550, XRD results confirmed the occurrence of hydroxyapatite (HAP) ($\text{Ca}_5(\text{PO}_4)_3(\text{OH})$) and calcite crystals (CaCO_3), validating FTIR findings on the nature of inorganic compounds present and providing further evidence on the fertiliser value and liming ability of SSF biochars. Overall, FTIR analysis coupled with XRD validation is suggested as a quick and reliable method to confirm the chemical composition, both amorphous and crystalline, of human excreta biochars.

3.3.3. Value as a solid fuel

The demand for sustainable alternatives to charcoal fuels is intensified by climate change and energy challenges, and can be (partially) met through waste biomass valorisation (Lohri et al., 2016). Nevertheless, FS-based solid fuels often have relatively low calorific values and cannot easily sustain the production of marketable briquettes that are competitive against traditional charcoal fuels, particularly for high-ash

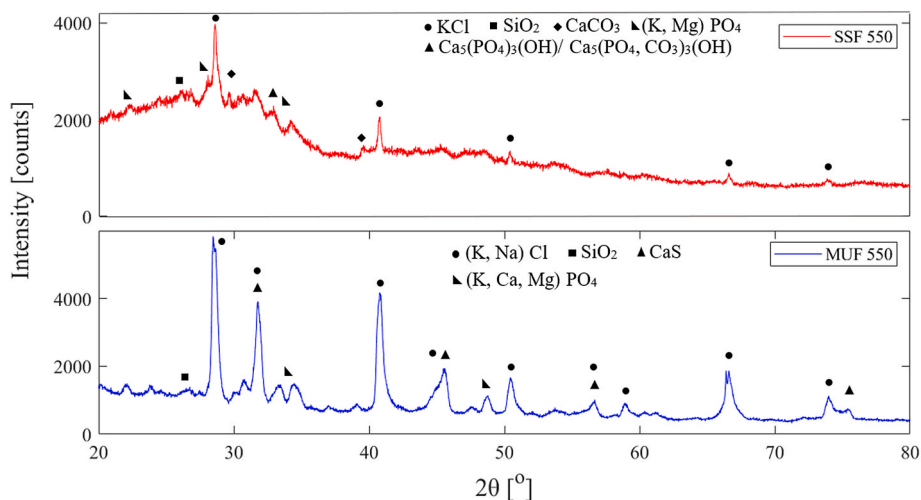


Fig. 4. X-ray diffraction (XRD) patterns for source-separated faeces (SSF) and mixed urine and faeces (MUF) biochars (produced at 550 °C).

FS sources. Source separation of human excreta can be investigated as a method to create more energy-dense excreta based solid fuels, along with the addition of other sources of biomass, like sawdust or agricultural waste, which has been previously established in the literature as a strategy to increase fuel calorific value and decrease ash, N and S content (Hafford et al., 2018; Hübner et al., 2019). It is evident that SSF biochars have significantly higher calorific values compared to MUF, notably 20.3 MJ/kg for SSF450 compared to 13.3 MJ/kg for MUF450, which corresponds to around 50% increase in calorific value density with source separation. Moreover, source separation allows for the combination of resource recovery objectives, as the urine stream would remain available for nutrient recovery.

For both SSF and MUF biochars, HHVs are lower after pyrolysis and further decrease with an increase of pyrolysis temperature from 450 °C to 550 °C (Table 1). No significant change in calorific value is noticed

between 550 °C and 650 °C. The pattern of calorific value decreasing with increasing temperature has also been noticed for faeces by Ward et al. (2014) and for FS by Gold et al. (2018). Therefore, within the studied temperature range, 450–500 °C is the most suitable for the production of excreta-based solid fuels, although this might change with the addition of other biomass sources in the feedstock mix. Lower temperatures (350–450 °C) can be considered when the production of solid fuels is the main objective, although char stability is unlikely to be established. In any case, the volatile matter content of char-based solid fuels should be monitored to ensure emissions during combustion are minimised (Falemara et al., 2018).

The lower S concentrations in SSF550 and SSF650 (Table 1) meet guiding values for the unproblematic combustion of solid fuels in terms of SO_x emissions (<0.2% S content), although these are not met for SSF450 or any of the MUF biochars (Oberberger et al., 2006). Both

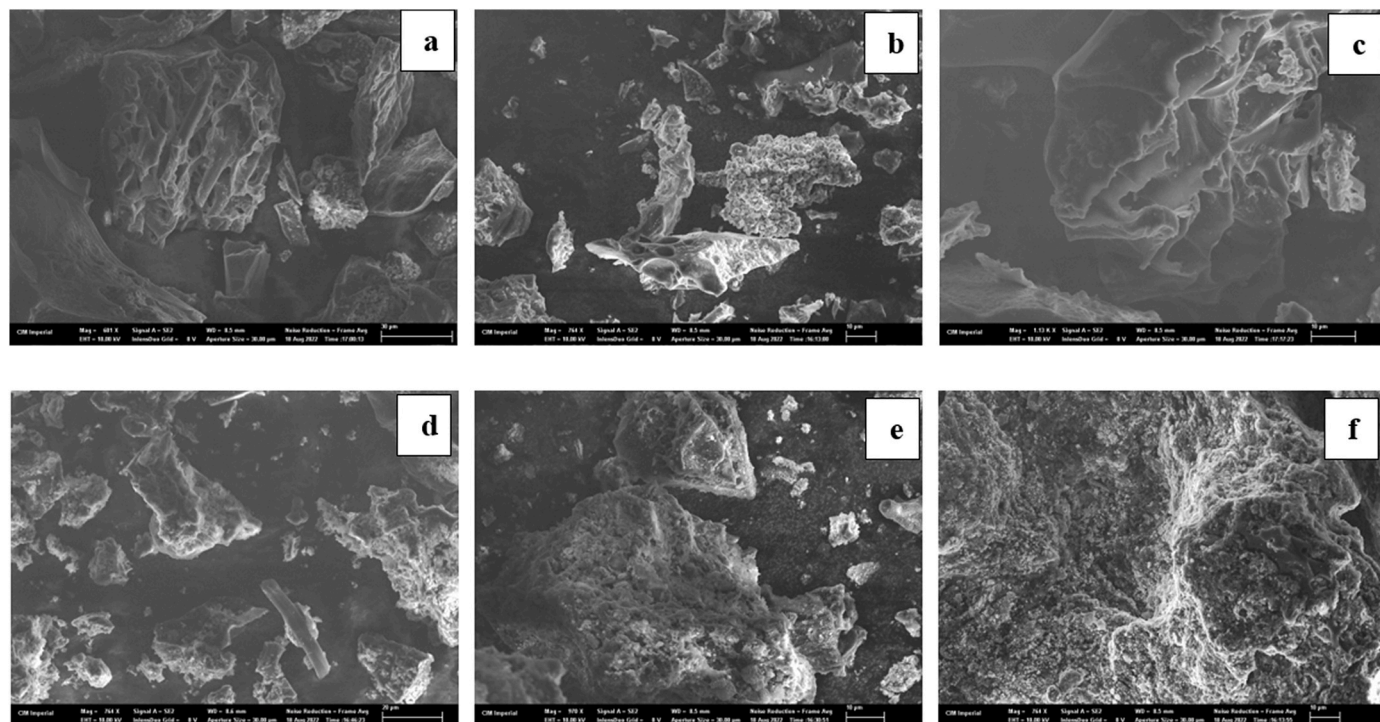


Fig. 5. Scanning Electron Microscopy (SEM) images for source-separated faeces (SSF) biochars: SSF550 (a), SSF650 (b, c); and mixed urine and faeces (MUF) biochars: MUF550 (d) and MUF650 (e, f).

types of biochars have higher N content than recommended values (<2.5–0.6%) which requires caution over NO_x emissions when burning excreta-based solid fuels (Gold et al., 2017). Therefore, the combination of excreta with other sources of biomass that have lower N and S concentrations compared to FS (e.g., wood), is essential not only to boost the final products' calorific value but also to limit combustion emissions (Hafford et al., 2018; Ippolito et al., 2020). When excreta-based chars are used to produce briquettes, it is recommended that the final products are tested for their composition and fuel characteristics, to ensure emissions and burning efficiency are optimised.

3.3.4. Surface morphology

SEM images of SSF and MUF biochars are shown in Fig. 5. A range of formations with different surface morphology can be observed. Notably Fig. 5b captures typical organic structures, as well as crystal-like shapes and porous mineral formations. Some crystal formations appear to be incorporated into the carbon matrix for SSF biochars, which was not observed for MUF (Fig. 5a, d). Interestingly, the surface of MUF biochars was more porous compared to SSF (Fig. 5e and f). MUF650 also presents a more developed pore structure compared to MUF550, which is in line with literature findings of biochar pore volume and surface area increasing with pyrolysis temperature (Ma et al., 2016; Nkomo et al., 2021). SSF biochars present a more sheet-like texture, with macroporous cavities which can be attributed to the decomposition of the faeces' organic structure (Fig. 5c) (Wildman and Derbyshire, 1991). Both types of biochar appear to have minerals present both on the surface as well as embedded in the carbon matrix, as indicated by the compositional contrast of the images, whereby minerals that have a higher atomic number than carbon appear brighter (Singh et al., 2017).

The images captured suggest that the addition of urine can significantly alter the surface morphology of produced biochars, which can partly be attributed to the introduction of free moisture on the feedstock surface. Dehydration reactions – occurring either during initial drying at high temperatures, like in this study, or at the onset of pyrolysis in cases of incomplete pre-drying – can cause the formation of richer pore canals and alter the surface structure of resulting biochars (Chen et al., 2022). It has previously been observed that the presence of moisture during sewage sludge pyrolysis can intensify devolatilisation processes and increase porosity (Xiong et al., 2013). The urine fraction is also rich in NH₄-N and K salts, which have been used as activation agents for biomass-derived chars (Moussavi et al., 2013; Zhu et al., 2018). Further investigation of the surface chemistry of source-separated and mixed-stream excreta based biochars could offer valuable insights on their comparative suitability as adsorbents and other related parameters, including their water holding capacity (Das and Ghosh, 2022). Nevertheless, the increased energy intensity and significant N losses (and emissions) associated with urine-containing sludge pyrolysis, should be balanced against any adsorption reuse benefits.

4. Conclusions

Overall, source separation is a promising source control method to increase resource recovery from human excreta pyrolysis. For the first time, this study has established a quantifiable relationship between human excreta source separation and biochar quality, under the prism of nutrient and energy recovery. Key findings are that:

- Impacts of source separation on the thermal decomposition behaviour of feedstocks can be attributed to differences in fat content and the nature of nitrogenous compounds present. Detailed characterisation of the major organic compounds (cellulose, hemicellulose, lignin, protein, oil and grease) in separated and non-separated human excreta is recommended to further investigate these effects and differences.

- Both SSF and MUF biochars were found to have good P recovery potential, with FTIR and XRD results validating the presence of phosphate compounds of high fertiliser value.
- Urine diversion significantly benefits N recovery (70% of total N losses during thermal treatment avoided) and results in SSF biochars with higher liming potential.
- Source-separated faeces produce more energy-dense fuels (50% increase in char calorific value), while allowing the combination of energy and nutrient recovery from faeces and urine respectively.
- Mixed excreta biochars are more PK-rich and have higher cation exchange capacity, but their high salinity may place limitations on their use in agriculture, especially for application to salt sensitive plants.
- Statistical analysis showed that source separation had a significant effect on all quantitative biochar parameters tested. Pyrolysis temperature also influenced biochar characteristics, with most statistically significant changes observed at the 450–550 °C range.
- Nutrient and carbon behaviour during pyrolysis suggested that temperatures around 500 °C can balance biochar stability, nutrient availability and solid fuel value objectives, for both separated and non-separated human excreta feedstocks.
- Effects of source separation on biochar surface morphology were qualitatively identified and higher porosity observed for MUF compared to SSF biochars. Further research is recommended to investigate practical impacts on different resource recovery applications.

5. Implications

Ultimately, resource recovery benefits (both financial and environmental) should act as an incentive to achieve safe sanitation for all, in line with the UN SDGs. To achieve SDG 6, a significant number of new on-site sanitation facilities needs to be installed and incorporated within sustainable FSM systems. While these topics are multi-dimensional and require a systems-thinking approach to be analysed, resource recovery is an important aspect of all sustainable sanitation systems. Apart from environmental benefits, it can create a much-needed revenue stream at the back-end of sanitation and FSM chains (Diener et al., 2014; Trimmer et al., 2019). Efforts to create resource recovery businesses from on-site sanitation systems are in place, but they are challenging from an economic perspective and usually rely on external funding and subsidies in order to be sustained (World Bank, 2019).

Establishing relationships between source control and end uses of recovered products can create pathways for the production of consistent, marketable excreta-based products. In turn, the operation of sanitation businesses that cover the entire FSM service chain encourages the correct use of container-based and source separating toilets by providing frequent collection and maintenance services for toilet users. Therefore, a reinforcing loop is created whereby improved sanitation services create more opportunities for resource recovery applications, and resource recovery benefits encourage the improved coverage and efficient use of sanitation systems. Further research is needed towards the urgent requirement of recovering resources from human excreta at full-scale and assessing the market-value and environmental benefits of the recovered products. Ultimately though, achieving safe sanitation for all is, and should be, the core of FSM research.

Credit author statement

Maria E. Koulouri: Conceptualisation, Investigation, Methodology, Formal analysis, Visualisation, Writing – original draft; **Michael R. Templeton:** Conceptualisation, Supervision, Writing – review & editing; **Geoffrey D. Fowler:** Conceptualisation, Supervision, Writing – review & editing.

Declaration of competing interest

The authors declare that they have no known competing financial interests or personal relationships that could have appeared to influence the work reported in this paper.

Data availability

Data will be made available on request.

Acknowledgements

The authors would like to thank the Department of Civil and Environmental Engineering of Imperial College London for the donation of a scholarship and the Society of Chemical Industry (SCI) for financially supporting this work. This project was also supported by the Royal Academy of Engineering under the Research Chairs and Senior Research Fellowships programme. Approvals and permissions for the collection of human excreta samples used in this research project were obtained via the Imperial College Research Governance and Integrity Team (RGIT ref. no. 21IC6817) and the Imperial College Healthcare Tissue Bank (ICHTB HTA licence: 12275) [supported by the National Institute for Health Research (NIHR) Biomedical Research Centre based at Imperial College Healthcare NHS Trust and Imperial College London].

Appendix A. Supplementary data

Supplementary data to this article can be found online at <https://doi.org/10.1016/j.jenvman.2023.117782>.

References

- APHA, 1992. *Standard Methods: for the Examination of Water and Wastewater*, eighteenth ed. American Public Health Association.
- ASTM, 2015. ASTM D7582-15 Standard: Standard Test Methods for Proximate Analysis of Coal and Coke by Macro Thermogravimetric Analysis. ASTM International. <https://doi.org/10.1520/D7582-15>.
- ASTM, 2019. Gross Calorific Value of Coal and Coke. ASTM International. https://doi.org/10.1520/D5865_D5865M-19. ASTM D5865/D5865M-19 Standard: Standard Test Method for.
- ASTM, 2021. Practice for General Techniques for Obtaining Infrared Spectra for Qualitative Analysis. ASTM International. <https://doi.org/10.1520/E1252-98R21>. ASTM E1252-98 (2021) Standard.
- Bleuler, M., Gold, M., Strande, L., Schönborn, A., 2020. Pyrolysis of dry toilet substrate as a means of nutrient recycling in agricultural systems: potential risks and benefits. *Waste Biomass Valorization* 12, 4171–4183. <https://doi.org/10.1007/s12649-020-01220-0>.
- Bond, T., Tse, Q., Chambon, C.L., Fennell, P., Fowler, G.D., Krueger, B.C., Templeton, M. R., 2018. The feasibility of char and bio-oil production from pyrolysis of pit latrine sludge. *Environ. Sci. Water Res. Technol.* 4, 253–264. <https://doi.org/10.1039/C7EW00380C>.
- Canfield, D.E., Glaser, A.N., Falkowski, P.G., 2010. The evolution and future of earth's nitrogen cycle. *Science* 330, 192–196. <https://doi.org/10.1126/science.1186120>.
- Chapman, H.D., 1965. Cation-exchange capacity. In: Norman, A.G. (Ed.), *Methods of Soil Analysis*. John Wiley & Sons, Ltd, pp. 891–901. <https://doi.org/10.2134/agronmonogr9.2.c6>.
- Chen, J., Gao, S., Xu, F., Xu, W., Yang, Y., Kong, D., Wang, Y., Yao, H., Chen, H., Zhu, Y., Mu, L., 2022. Influence of moisture and feedstock form on the pyrolysis behaviors, pyrolytic gas production, and residues micro-structure evolutions of an industrial sludge from a steel production enterprise. *Energy* 248, 123603. <https://doi.org/10.1016/j.energy.2022.123603>.
- Chipako, T.L., Randall, D.G., 2020. Urine treatment technologies and the importance of pH. *J. Environ. Chem. Eng.* 8, 103622 <https://doi.org/10.1016/j.jece.2019.103622>.
- Cordell, D., Drangert, J.-O., White, S., 2009. The story of phosphorus: global food security and food for thought. *Global Environ. Change* 19, 292–305. <https://doi.org/10.1016/j.gloenvcha.2008.10.009>.
- Das, S.K., Ghosh, G.K., 2021. Developing biochar-based slow-release N-P-K fertilizer for controlled nutrient release and its impact on soil health and yield. *Biomass Convers. Biorefinery*. <https://doi.org/10.1007/s13399-021-02069-6>.
- Das, S.K., Ghosh, G.K., 2022. Soil hydro-physical properties affected by biomass-derived biochar and organic manure: a low-cost technology for managing acidic mountain sandy soils of north eastern region of India. *Biomass Convers. Biorefinery*. <https://doi.org/10.1007/s13399-022-03107-7>.
- De Koninck, A.-S., Nys, K., Vandenheede, B., Van Biervliet, S., Speckaert, M.M., Delanghe, J.R., 2016. Detailed faecal fat analysis using Fourier transform infrared spectroscopy: exploring the possibilities. *Clin. Biochem.* 49, 1283–1287. <https://doi.org/10.1016/j.clinbiochem.2016.07.017>.
- Diener, S., Semiyaga, S., Niwagaba, C.B., Muspratt, A.M., Gning, J.B., Mbéguéré, M., Ennin, J.E., Zurbrugg, C., Strande, L., 2014. A value proposition: resource recovery from faecal sludge—can it be the driver for improved sanitation? *Resour. Conserv. Recycl.* 88, 32–38. <https://doi.org/10.1016/j.resconrec.2014.04.005>.
- EBC, 2012. European Biochar Certificate - Guidelines for a Sustainable Production of Biochar. European Biochar Foundation. <https://doi.org/10.13140/RG.2.1.4658.7043>. Version 6.1 of 19th June 2015.
- Falemara, B.C., Joshua, V.I., Aina, O.O., Nuhu, R.D., 2018. Performance evaluation of the physical and combustion properties of briquettes produced from agro-wastes and wood residues. *Recycling* 3, 37. <https://doi.org/10.3390/recycling3030037>.
- Fidalgo, B., Chilmeran, M., Somorin, T., Sowale, A., Kolios, A., Parker, A., Williams, L., Collins, M., McAdam, E.J., Tyrrel, S., 2019. Non-isothermal thermogravimetric kinetic analysis of the thermochemical conversion of human faeces. *Renew. Energy* 132, 1177–1184. <https://doi.org/10.1016/j.renene.2018.08.090>.
- Figueiredo, C.C. de, Reis, A. de S.P.J., Araujo, A.S. de, Blum, L.E.B., Shah, K., Paz-Ferreiro, J., 2021. Assessing the potential of sewage sludge-derived biochar as a novel phosphorus fertilizer: influence of extractant solutions and pyrolysis temperatures. *Waste Manag.* 124, 144–153. <https://doi.org/10.1016/j.wasman.2021.01.044>.
- Galván-Ruiz, M., Hernández, J., Baños, L., Noriega-Montes, J., Rodríguez-García, M.E., 2009. Characterization of calcium carbonate, calcium oxide, and calcium hydroxide as starting point to the improvement of lime for their use in construction. *J. Mater. Civ. Eng.* 21, 694–698. ASCE/0899-1561(2009)21:11(694), 10.1061/.
[https://doi.org/10.1061/ASCE/0899-1561\(2009\)21:11\(694\)](https://doi.org/10.1061/ASCE/0899-1561(2009)21:11(694)).
- Glaser, B., Lehr, V.-I., 2019. Biochar effects on phosphorus availability in agricultural soils: a meta-analysis. *Sci. Rep.* 9, 9338. <https://doi.org/10.1038/s41598-019-45693-z>.
- Gold, M., Ddiba, D.I.W., Seck, A., Sekigongo, P., Diene, A., Diaw, S., Niang, S., Niwagaba, C., Strande, L., 2017. Faecal sludge as a solid industrial fuel: a pilot-scale study. *J. Water, Sanit. Hyg. Dev.* 7, 243–251. <https://doi.org/10.2166/washdev.2017.089>.
- Gold, M., Cunningham, M., Bleuler, M., Arnheiter, R., Schönborn, A., Niwagaba, C., Strande, L., 2018. Operating parameters for three resource recovery options from slow-pyrolysis of faecal sludge. *J. Water, Sanit. Hyg. Dev.* 8, 707–717. <https://doi.org/10.2166/washdev.2018.009>.
- Guest, J.S., Skerlos, S.J., Barnard, J.L., Beck, M.B., Daigger, G.T., Hilger, H., Jackson, S. J., Karvazy, K., Kelly, L., Macpherson, L., Mihelcic, J.R., Pramanik, A., Raskin, L., Van Loosdrecht, M.C.M., Yeh, D., Love, N.G., 2009. A new planning and design paradigm to achieve sustainable resource recovery from wastewater. *Environ. Sci. Technol.* 43, 6126–6130. <https://doi.org/10.1021/es9010515>.
- Hafford, L.M., Ward, B.J., Weimer, A.W., Linden, K., 2018. Fecal sludge as a fuel: characterization, cofire limits, and evaluation of quality improvement measures. *Water Sci. Technol.* 78, 2437–2448. <https://doi.org/10.2166/wst.2019.005>.
- Haris, P.I., Severcan, F., 1999. FTIR spectroscopic characterization of protein structure in aqueous and non-aqueous media. *J. Mol. Catal. B Enzym.* 7, 207–221. [https://doi.org/10.1016/S1381-1177\(99\)00030-2](https://doi.org/10.1016/S1381-1177(99)00030-2).
- Hossain, M.K., Strezov, V., Chan, K.Y., Ziolkowski, A., Nelson, P.F., 2011. Influence of pyrolysis temperature on production and nutrient properties of wastewater sludge biochar. *J. Environ. Manag.* 92, 223–228. <https://doi.org/10.1016/j.jenvman.2010.09.008>.
- Hseu, Z.-Y., 2004. Evaluating heavy metal contents in nine composts using four digestion methods. *Bioresour. Technol.* 95, 53–59. <https://doi.org/10.1016/j.biortech.2004.02.008>.
- Hübner, T., Herrmann, A., Kretzschmar, J., Harnisch, F., 2019. Suitability of fecal sludge from composting toilets as feedstock for carbonization. *J. Water, Sanit. Hyg. Dev.* 9, 616–626. <https://doi.org/10.2166/washdev.2019.047>.
- IBI, 2015. International Biochar Initiative - Standardized Product Definition and Product Testing Guidelines for Biochar that Is Used in Soil. Version 2.1. <https://biochar-international.org/characterizationstandard/>.
- Ippolito, J.A., Spokas, K.A., Novak, J.M., Lentz, R.D., Cantrell, K.B., 2015. Biochar elemental composition and factors influencing nutrient retention. In: Lehmann, J., Joseph, S. (Eds.), *Biochar for Environmental Management: Science, Technology and Implementation*, second ed. Routledge, pp. 139–164. <https://doi.org/10.4324/9780203762264>.
- Ippolito, J.A., Cui, L., Kammann, C., Wrage-Mönnig, N., Estavillo, J.M., Fuertes-Mendizabal, T., Cayuela, M.L., Sigua, G., Novak, J., Spokas, K., Borchard, N., 2020. Feedstock choice, pyrolysis temperature and type influence biochar characteristics: a comprehensive meta-data analysis review. *Biochar* 2, 421–438. <https://doi.org/10.1007/s42773-020-00067-x>.
- Ismail, S., Ali, E., Alwan, B., Abd, A., 2022. Potassium chloride nanoparticles: synthesis, characterization, and study the antimicrobial applications. *Macromol. Symp.* 401, 2100312 <https://doi.org/10.1002/masy.202100312>.
- ISO, 2015. ISO 16948:2015: Solid Biofuels. Determination of Total Content of Carbon, Hydrogen and Nitrogen. International Organization for Standardization. <https://www.iso.org/standard/58004.html>.
- Jastrzębski, W., Sitarz, M., Rokita, M., Bulat, K., 2011. Infrared spectroscopy of different phosphates structures. *Spectrochim. Acta. A. Mol. Biomol. Spectrosc.* 79, 722–727. <https://doi.org/10.1016/j.saa.2010.08.044>.
- Jones, G.C., Jackson, B., 1993. Infrared Transmission Spectra of Carbonate Minerals. Springer Netherlands, Dordrecht. <https://doi.org/10.1007/978-94-011-2120-0>.
- Jones, J.M., Rollinson, A.N., 2013. Thermogravimetric evolved gas analysis of urea and urea solutions with nickel alumina catalyst. *Thermochim. Acta* 565, 39–45. <https://doi.org/10.1016/j.tca.2013.04.034>.
- Krounbi, L., Es, H., Karanja, N., Lehmann, J., 2018. Nitrogen and phosphorus availability of biologically and thermochemically decomposed human wastes and urine in soils

- with different texture and pH. *Soil Sci.* 183, 51–65. <https://doi.org/10.1097/SS.0000000000000229>.
- Krounbi, L., Enders, A., van Es, H., Woolf, D., von Herzen, B., Lehmann, J., 2019. Biological and thermochemical conversion of human solid waste to soil amendments. *Waste Manag.* 89, 366–378. <https://doi.org/10.1016/j.wasman.2019.04.010>.
- Krueger, B.C., Fowler, G.D., Templeton, M.R., Moya, B., 2020. Resource recovery and biochar characteristics from full-scale faecal sludge treatment and co-treatment with agricultural waste. *Water Res.* 169, 115253 <https://doi.org/10.1016/j.watres.2019.115253>.
- Krueger, B.C., Fowler, G.D., Templeton, M.R., 2021a. Critical analytical parameters for faecal sludge characterisation informing the application of thermal treatment processes. *J. Environ. Manag.* 280, 111658 <https://doi.org/10.1016/j.jenvman.2020.111658>.
- Krueger, B.C., Fowler, G.D., Templeton, M.R., Septien, S., 2021b. Faecal sludge pyrolysis: understanding the relationships between organic composition and thermal decomposition. *J. Environ. Manag.* 298, 113456 <https://doi.org/10.1016/j.jenvman.2021.113456>.
- Kwon, E.E., Lee, T., Ok, Y.S., Tsang, D.C.W., Park, C., Lee, J., 2018. Effects of calcium carbonate on pyrolysis of sewage sludge. *Energy* 153, 726–731. <https://doi.org/10.1016/j.energy.2018.04.100>.
- Larsen, T.A., Udert, K., Lienert, J., 2013. *Source Separation and Decentralization for Wastewater Management*. IWA Publishing. <https://doi.org/10.2166/9781780401072>.
- Larsen, T.A., 2020. Urine source separation for global nutrient management. In: O'Bannon, D.J. (Ed.), *Women in Water Quality: Investigations by Prominent Female Engineers, Women in Engineering and Science*. Springer International Publishing, Cham, pp. 99–111. https://doi.org/10.1007/978-3-030-17819-2_6.
- Lehmann, J., Joseph, S., 2015. *Biochar for Environmental Management: Science, Technology and Implementation*. Taylor & Francis Group. <https://doi.org/10.4324/9780203762264>.
- Liu, X., Li, Z., Zhang, Y., Feng, R., Mahmood, I.B., 2014. Characterization of human manure-derived biochar and energy-balance analysis of slow pyrolysis process. *Waste Manag.* 34, 1619–1626. <https://doi.org/10.1016/j.wasman.2014.05.027>.
- Lohri, C.R., Rajabu, H.M., Sweeney, D.J., Zurbrugg, C., 2016. Char fuel production in developing countries – a review of urban biowaste carbonization. *Energy Res.* 59, 1514–1530. <https://doi.org/10.1016/j.rser.2016.01.088>.
- Ma, X., Zhou, B., Budai, A., Jeng, A., Hao, X., Wei, D., Zhang, Y., Rasse, D., 2016. Study of biochar properties by scanning electron microscope – energy dispersive X-ray spectroscopy (SEM-EDX). *Commun. Soil Sci. Plant Anal.* 47, 593–601. <https://doi.org/10.1080/00103624.2016.1146742>.
- Méndez, A., Terradillos, M., Gascó, G., 2013. Physicochemical and agronomic properties of biochar from sewage sludge pyrolysed at different temperatures. *J. Anal. Appl. Pyrolysis* 102, 124–130. <https://doi.org/10.1016/j.jaap.2013.03.006>.
- Moussavi, G., Alahabadi, A., Yaghmaei, K., Eskandari, M., 2013. Preparation, characterization and adsorption potential of the NH₄Cl-induced activated carbon for the removal of amoxicillin antibiotic from water. *Chem. Eng. J.* 217, 119–128. <https://doi.org/10.1016/j.cej.2012.11.069>.
- Munera-Echeverri, J.L., Martinsen, V., Strand, L.T., Zivanovic, V., Cornelissen, G., Mulder, J., 2018. Cation exchange capacity of biochar: an urgent method modification. *Sci. Total Environ.* 642, 190–197. <https://doi.org/10.1016/j.scitotenv.2018.06.017>.
- Nkomo, N., Odindo, A.O., Musazura, W., Missengue, R., 2021. Optimising pyrolysis conditions for high-quality biochar production using black soldier fly larvae faecal-derived residue as feedstock. *Heliyon* 7, e07025. <https://doi.org/10.1016/j.heliyon.2021.e07025>.
- Oberberger, I., Brunner, T., Bärnthaler, G., 2006. Chemical properties of solid biofuels—significance and impact. *Biomass Bioenergy* 30, 973–982. <https://doi.org/10.1016/j.biombioe.2006.06.011>.
- Orner, K.D., Mihelcic, J.R., 2017. A review of sanitation technologies to achieve multiple sustainable development goals that promote resource recovery. *Environ. Sci. Water Res. Technol.* 4, 16–32. <https://doi.org/10.1039/C7EW00195A>.
- Pradel, M., Aissani, L., Villot, J., Baudez, J.-C., Laforest, V., 2016. From waste to added value product: towards a paradigm shift in life cycle assessment applied to wastewater sludge – a review. *J. Clean. Prod.* 131, 60–75. <https://doi.org/10.1016/j.jclepro.2016.05.076>.
- Rehman, I., Bonfield, W., 1997. Characterization of hydroxyapatite and carbonated apatite by photo acoustic FTIR spectroscopy. *J. Mater. Sci. Mater. Med.* 8, 1–4. <https://doi.org/10.1023/A:1018570213546>.
- Ren, N., Tang, Y., Li, M., 2018. Mineral additive enhanced carbon retention and stabilization in sewage sludge-derived biochar. *Process Saf. Environ.* 115, 70–78. <https://doi.org/10.1016/j.psep.2017.11.006>.
- Rose, C., Parker, A., Jefferson, B., Cartmell, E., 2015. The characterization of feces and urine: a review of the literature to inform advanced treatment technology. *Crit. Rev. Environ. Sci. Technol.* 45, 1827–1879. <https://doi.org/10.1080/10643389.2014.1000761>.
- Shapaval, V., Brandenburg, J., Blomqvist, J., Tafintseva, V., Passoth, V., Sandgren, M., Kohler, A., 2019. Biochemical profiling, prediction of total lipid content and fatty acid profile in oleaginous yeasts by FTIR spectroscopy. *Biotechnol. Biofuels* 12, 140. <https://doi.org/10.1186/s13068-019-1481-0>.
- Singh, B., Camps-Arbestain, M., Lehmann, J., 2017. *Biochar: A Guide to Analytical Methods*. Csiro Publishing. <https://doi.org/10.1071/9781486305100>.
- Smidt, E., Schwanninger, M., 2005. Characterization of waste materials using FTIR spectroscopy: process monitoring and quality assessment. *Spectrosc. Lett.* 38, 247–270. <https://doi.org/10.1081/SL-200042310>.
- Somorin, T., Parker, A., McAdam, E., Williams, L., Tyrrel, S., Kolios, A., Jiang, Y., 2020. Pyrolysis characteristics and kinetics of human faeces, simulant faeces and wood biomass by thermogravimetry–gas chromatography–mass spectrometry methods. *Energy Rep.* 6, 3230–3239. <https://doi.org/10.1016/j.egy.2020.11.164>.
- Stanislavov, A.S., Sukhodub, L.F., Sukhodub, L.B., Kuznetsov, V.N., Bychkov, K.L., Kravchenko, M.I., 2018. Structural features of hydroxyapatite and carbonated apatite formed under the influence of ultrasound and microwave radiation and their effect on the bioactivity of the nanomaterials. *Ultrason. Sonochem.* 42, 84–96. <https://doi.org/10.1016/j.ulsonch.2017.11.011>.
- Strande, L., Ronteltap, M., Brdjanovic, D., 2014. *Faecal Sludge Management: Systems Approach for Implementation and Operation*. IWA Publishing. <https://doi.org/10.2166/9781780404738>.
- Strande, L., Schoebitz, L., Bischoff, F., Ddiba, O., Okello, F., Englund, M., Ward, B.J., Niwagaba, C.B., 2018. Methods to reliably estimate faecal sludge quantities and qualities for the design of treatment technologies and management solutions. *J. Environ. Manag.* 223, 898–907. <https://doi.org/10.1016/j.jenvman.2018.06.100>.
- Takagi, H., Maruyama, K., Yoshizawa, N., Yamada, Y., Sato, Y., 2004. XRD analysis of carbon stacking structure in coal during heat treatment. *Fuel* 83, 2427–2433. <https://doi.org/10.1016/j.fuel.2004.06.019>.
- Trimmer, J.T., Cusick, R.D., Guest, J.S., 2017. Amplifying progress toward multiple development goals through resource recovery from sanitation. *Environ. Sci. Technol.* 51, 10765–10776. <https://doi.org/10.1021/acs.est.7b02147>.
- Trimmer, J.T., Miller, D.C., Guest, J.S., 2019. Resource recovery from sanitation to enhance ecosystem services. *Nat. Sustain.* 2, 681–690. <https://doi.org/10.1038/s41893-019-0313-3>.
- US EPA, 1995. *Composite Sampling*. In: EPA Observational Economy Series, vol. 1. United States Environmental Protection Agency, Washington, DC.
- US EPA, 1996. *Method 3050B: Acid Digestion of Sediments, Sludges, and Soils. Revision 2*. United States Environmental Protection Agency, Washington, DC.
- Velkushanova, K., Strande, L., Ronteltap, M., Koottatep, T., Brdjanovic, D., Buckley, C. (Eds.), 2021. *Methods for Faecal Sludge Analysis*. IWA Publishing. <https://doi.org/10.2166/9781780409122>.
- Wang, T., Camps-Arbestain, M., Hedley, M., Bishop, P., 2012. Predicting phosphorus bioavailability from high-ash biochars. *Plant Soil* 357, 173–187. <https://doi.org/10.1007/s11104-012-1131-9>.
- Ward, B.J., Jacob, T.W., Montoya, L.D., 2014. Evaluation of solid fuel char briquettes from human waste. *Environ. Sci. Technol.* 48, 9852–9858. <https://doi.org/10.1021/es500197h>.
- WHO/UNICEF, 2021. *Progress on Household Drinking Water, Sanitation and Hygiene 2000–2020: Five Years into the SDGs*. World Health Organization (WHO) and the United Nations Children's Fund (UNICEF), Geneva.
- Wildman, J., Derbyshire, F., 1991. Origins and functions of macroporosity in activated carbons from coal and wood precursors. *Fuel* 70, 655–661. [https://doi.org/10.1016/0016-2361\(91\)90181-9](https://doi.org/10.1016/0016-2361(91)90181-9).
- Woldetsadik, D., Drechsel, P., Marschner, B., Itanna, F., Gebrekidan, H., 2017. Effect of biochar derived from faecal matter on yield and nutrient content of lettuce (*Lactuca sativa*) in two contrasting soils. *Environ. Syst. Res.* 6, 2. <https://doi.org/10.1186/s40068-017-0082-9>.
- World Bank, 2012. *What a Waste: A Global Review of Solid Waste Management*. Urban Development Series; Knowledge Papers No. 15. World Bank, Washington, DC. <https://openknowledge.worldbank.org/handle/10986/17388>.
- World Bank, 2019. *Evaluating the Potential of Container-Based Sanitation: Sanergy in Nairobi, Kenya*. World Bank, Washington, DC. <http://documents.worldbank.org/curated/en/661201550180019891/Evaluating-the-Potential-of-Container-Based-Sanitation-Sanergy-in-Nairobi-Kenya>.
- Xiong, S., Zhuo, J.-K., Zhang, B., Yao, Q., 2013. Effect of moisture content on the characterization of products from the pyrolysis of sewage sludge. *J. Anal. Appl. Pyrolysis* 104, 632–639. <https://doi.org/10.1016/j.jaap.2013.05.003>.
- Zhu, L., Zhao, N., Tong, L., Lv, Y., 2018. Structural and adsorption characteristics of potassium carbonate activated biochar. *RSC Adv.* 8, 21012–21019. <https://doi.org/10.1039/C8RA03335H>.
- Zhu, N., Qian, F., Xu, X., Wang, M., Teng, Q., 2021. Thermogravimetric experiment of urea at constant temperatures. *Materials* 14, 6190. <https://doi.org/10.3390/ma14206190>.